Published OnlineFirst April 25, 2013; DOI: 10.1158/1535-7163.MCT-12-0988

Large Molecule Therapeutics

Molecular Cancer Therapeutics

Human Anti-Macrophage Migration Inhibitory Factor Antibodies Inhibit Growth of Human Prostate Cancer Cells *In Vitro* and *In Vivo*

Filza Hussain[1], Michael Freissmuth[1], Dirk Völkel[2], Michael Thiele[2], Patrice Douillard[2], Gerhard Antoine[2], Patrick Thurner[1], Hartmut Ehrlich[2], Hans-Peter Schwarz[2], Friedrich Scheiflinger[2], and Randolf J. Kerschbaumer[2]

Abstract

Macrophage migration inhibitory factor (MIF) is a proinflammatory cytokine, originally discovered for its eponymous effect and now known for pleiotropic biologic properties in immunology and oncology. Circulating MIF levels are elevated in several types of human cancer including prostate cancer. MIF is released presumably by both stromal and tumor cells and enhances malignant growth and metastasis by diverse mechanisms, such as stimulating tumor cell proliferation, suppressing apoptotic death, facilitating invasion of the extracellular matrix, and promoting angiogenesis. Recently described fully human anti-MIF antibodies were tested *in vitro* and *in vivo* for their ability to influence growth rate and invasion of the human PC3 prostate cancer cell line. *In vitro*, the selected candidate antibodies BaxG03, BaxB01, and BaxM159 reduced cell growth and viability by inhibiting MIF-induced phosphorylation of the central kinases p44/42 mitogen-activated protein kinase [extracellular signal–regulated kinase-1 and -2 (ERK1/2)] and protein kinase B (AKT). Incubation of cells in the presence of the antibodies also promoted activation of caspase-3/7. The antibodies furthermore inhibited MIF-promoted invasion and chemotaxis as transmigration through Matrigel along a MIF gradient was impaired. *In vivo*, pharmacokinetic parameters (half-life, volume of distribution, and bioavailability) of the antibodies were determined and a proof-of-concept was obtained in a PC3-xenograft mouse model. Treatment with human anti-MIF antibodies blunted xenograft tumor growth in a dose-dependent manner. We therefore conclude that the anti-MIF antibodies described neutralize some of the key tumor-promoting activities of MIF and thus limit tumor growth *in vivo*. *Mol Cancer Ther; 12(7); 1223–34. ©2013 AACR.*

Introduction

Macrophage migration inhibitory factor (MIF) was originally discovered as an activity released by antigen-stimulated lymphocytes some 45 years ago (1, 2). MIF is a proinflammatory cytokine and a counter-regulator of glucocorticoids. Many aspects of the biology of MIF are still shrouded in mystery. MIF lacks an N-terminal signal peptide and is secreted in a poorly understood, atypical fashion (3). The central portion of MIF contains a CXXC motif (^{57}Cys-Ala-Leu-Cys^{60}) present in thioredoxin and other thiol-protein-oxidoreductases. In fact, MIF displays oxidoreductase catalytic activity, which is responsible for some of its biologic effects (4). In addition, MIF catalyzes the conversion of dopachrome to 5,6-dihydroxyindole-2-carboxylic acid (5). However, this tautomerase activity is currently considered of modest biologic relevance (6). MIF is thought to bind to a cell surface receptor comprising CD74 (the invariant chain associated with MHC class II molecules) and CD44 (the cell surface receptor for hyaluronic acid; ref. 7). More recently, G protein–coupled chemokine receptors [the interleukin (IL)-8 receptor CXCR2, the stromal-derived factor-1 receptors CXCR4 and CXCR7] were proposed to act as MIF-receptors (8–10). However, the precise composition and functional profile of MIF/receptor complexes is not known (11). In addition, MIF may also elicit effects via intracellular sites of action: MIF is internalized and binds to cytosolic proteins, most prominently JUN-activation domain-binding protein 1/COP9 signalosome subunit 5 (JAB1/CSN5; refs. 12, 13).

Extracellular MIF is thought to play a role in tumor growth via several mechanisms. (i) MIF acts directly on tumor cells by activating signaling pathways that promote cell proliferation and cell survival. Extracellular MIF stimulates signaling cascades that lead to activation of

Authors' Affiliations: [1]Institute of Pharmacology, Centre of Physiology and Pharmacology, Medical University Vienna, Vienna; and [2]Baxter Biomedical Research Center, Baxter Innovations GmbH, Orth and der Donau, Austria

Note: Supplementary data for this article are available at Molecular Cancer Therapeutics Online (http://mct.aacrjournals.org/).

Corresponding Author: Michael Freissmuth, Institute of Pharmacology, Center of Physiology and Pharmacology, Medical University Vienna, Währinger Str. 13a, 1090 Vienna, Austria. Phone: 43-1-4277-64171; Fax: 43-1-4277-9641; E-mail: michael.freissmuth@meduniwien.ac.at

doi: 10.1158/1535-7163.MCT-12-0988

Published OnlineFirst April 25, 2013; DOI: 10.1158/1535-7163.MCT-12-0988

kinases, in particular p44/42 mitogen-activated protein kinase (extracellular signal–regulated kinase-1 and -2, ERK1/2) and protein kinase B/AKT (12, 14, 15). MIF exerts antiapoptotic effects by inhibition of p53 (16). This leads to accumulation of DNA mutations and favors tumor formation. (ii) MIF facilitates invasion of the extracellular matrix and induces angiogenesis and tumor vascularization by upregulating matrix metalloproteinases and proangiogenic factors such as VEGF, and IL-8 (17–19) and by controlling levels of hypoxia-inducible factor-1α (HIF-1α; ref. 20). (iii) In addition, as a secreted proinflammatory cytokine, MIF may be one of the mediators of tumor micro-inflammation (21). This concept has been revived to account for the fact that tumor cells can subvert inflammatory signals to promote their growth. In fact, ovarian cancer cells can exploit secreted MIF to escape immunosurveillance (22).

The importance of extracellular MIF for tumor development is further substantiated by the observation that MIF is released by several types of human cancer cells and elevated circulating levels are found in many patients (15). This is, in particular, true for prostate cancer, where expression of MIF is elevated (23), circulating MIF levels are correlated with poor prognosis (24), and where certain haplotypes arising from polymorphisms in the MIF promoter are associated with increased risk of prostate cancer (25). Blockage of MIF production or of its receptor CD74 blunts growth of prostate carcinoma cells (26). However, it has been speculated that intracellular MIF might have beneficial properties in cancer (27). Accordingly, MIF ought to represent an excellent target for antibodies, because they preclude the growth-promoting effect of released MIF but do not interfere with the intracellular effects of MIF. We explored this hypothesis by testing monoclonal antibodies directed against MIF on human prostate cancer cells *in vitro* and by verifying the effectiveness of these antibodies *in vivo* in a mouse PC3-xenograft model. We applied human anti-MIF antibodies that were recently described to exert MIF-neutralizing properties *in vitro* and in inflammatory disease models (28).

Materials and Methods

Materials

RPMI-1640 medium with 2 mmol/L L-glutamine was from PAA Laboratories, fetal calf serum (FCS) and Lipofectamine from GIBCO-Invitrogen, Accutase from Chemicon-Millipore, the Trypan blue solution (4%) from Sigma-Aldrich, materials for PAGE from Bio-Rad, nitrocellulose membranes for protein blotting from Schleicher & Schuell, anti-rabbit and anti-mouse immunoglobulins conjugated to horseradish peroxidase (HRP) from Amersham Biosciences, and the chemoluminescence substrate from Pierce. The following polyclonal antisera were from Cell Signaling Technology: antisera recognizing phospho-Thr^{308}-AKT, phospho-Ser^{473}-AKT, total AKT, dually phosphorylated (pThr^{202}-pTyr^{204}) ERK1/2, total ERK1/2, phospho-Thr^{125}-caspase-9, and total caspase-9. The fluorogenic caspase-3/7 substrate Ac-DEVD-AFC and caspase inhibitor Ac-DEVD-CHO were from Alexis Biochemicals, Matrigel from BD Biosciences, MaxiSorp ELISA plates from NUNC A/S, and ELISA reagents from Sigma. The avidin–biotin–blocking system and mouse immunoglobulin blocking reagents were from Vector Laboratories, IDetect super stain system HRP and aminoethylcarbazole kit from ID Labs, human Ki67 antibody from Dako. Transwell culture plates with 8-μm pore size were from Corning. The plasmid encoding enhanced GFP (pEGFP-C1) was from Clonetech. MF-1 nude mice were obtained from Harlan.

Protein purification

Human monoclonal antibodies BaxB01, BaxG03, and BaxM159 directed against MIF and an isotype-matched [immunoglobulin G1 (IgG1)] human control antibody were produced in stably transfected Chinese hamster ovary cells and were purified as described previously (28). Recombinant human MIF was expressed in *Escherichia coli* and purified from bacterial lysates (28); details of the purification strategy are described in the Supplementary Data.

Cell culture

PC-3 cells [American Type Culture Collection (ATCC) no. CRL-1435] and Du145 (ATCC no. HTB-81) were obtained from ATCC in 2008. These cell lines are authenticated on the basis of short-tandem repeats (listed in the ATCC catalog). Cell lines were cultured in RPMI-1640 medium supplemented with 10% FCS and 2 mmol/L glutamine at 37°C in a humidified incubator with 5% CO_2. Stocks were prepared after passage 3 and stored in liquid nitrogen. Cells were used up to passage 6 ($\leq$8 weeks in continuous culture) without further authentication. For some migration assays (see later), cells were transfected with a plasmid driving the expression of GFP using Lipofectamine and subjected to selection by geneticin (G418).

Growth inhibition

Cells were plated at 2.5×10^5 per 60-mm dish in triplicate and allowed to adhere for 24 hours. Thereafter, the medium was replaced with serum- and phenol red-free medium. After 24 hours, fresh medium containing 10% FCS and different concentrations of monoclonal antibodies was added. Cells were allowed to proliferate for another 24 hours. Subsequently, cells were washed with PBS, harvested by treatment with Accutase, and counted using a hematocytometer as a 50% suspension mixed with Trypan blue. Only viable (i.e., unstained, Trypan blue-excluding) cells were counted.

Immunoblotting

PC3 cells ($\sim 2 \times 10^5$/well) were seeded in 6-well dishes and starved as outlined earlier. Thereafter, cells were incubated for 48 hours in the presence of 10% FCS or the combination of 10% FCS with 100 nmol/L BaxG03, BaxB01, BaxM159, or the isotype control antibody. In some

Published OnlineFirst April 25, 2013; DOI: 10.1158/1535-7163.MCT-12-0988

instances, the medium contained 10 nmol/L recombinant MIF. After 48 hours, cells were lysed by the addition of boiling Laemmli buffer containing 100 mmol/L dithiothreitol (DTT) (1 mL/10 cm dish). The cell lysate was heated again to 95°C for 5 minutes, sonicated and cleared by centrifugation. Aliquots (20 μL) were applied to SDS-PAGE, the resolved proteins electrophoretically transferred onto nitrocellulose membranes, and the immunoreactive bands detected by enhanced chemiluminescence using the antibodies indicated in the figure legends.

Determination of caspase-3 activity

PC3 cells were seeded onto 10-cm culture dishes ($\sim 10^6$/dish) in the presence of 10% FCS (in RPMI-1640 containing phenol red and 2 mmol/L glutamine). After 24 hours, fresh medium was added containing the antibodies and recombinant MIF. After an incubation of another 48 hours, the cells were washed twice with ice-cold PBS. Lysis buffer (25 mmol/L HEPES·NaOH, pH 7.4, 5 mmol/L EDTA, 1 mmol/L EGTA, 5 mmol/L $MgCl_2$, 4 mmol/L DTT, and a protease inhibitor cocktail comprising aprotinin, pefablock, and leupeptin) was added onto the dishes (0.5 mL/dish), which were immersed in liquid N_2. After thawing, the suspension was transferred to Eppendorf tubes, again subjected to a freeze–thaw cycle, sonicated, and centrifuged at 12,000 × *g* (4°C, 20 minutes). Protein concentration in the supernatant was measured with Coomassie Brilliant Blue (reagent from Bio-Rad). The caspase reaction was monitored in a final volume of 0.1 mL containing supernatant (40 μg) and reaction buffer (40 mmol/L HEPES·NaOH, pH 7.4, 10% glycerol, 4 mmol/L DTT, and 50 μmol/L Ac-DEVD-AFC as the caspase-3 fluorogenic substrate) at 30°C using a PerkinElmer VICTOR3 Multilabel Counter (model 1420). Readings were obtained every 10 minutes for 3 hours with excitation set at 400 nm and emission recorded at 505 nm. To verify the specificity of the reaction, lysates were preincubated for 30 minutes at 30°C in the presence of the irreversible caspase-3 inhibitor Ac-DEVD-CHO (100 μmol/L) before addition of the substrate. Assays were done in triplicate.

Migration/invasion assay

Transwell dishes were coated on their lower side with poly-D-lysine. Subsequently, the upper side was covered with a thin layer of Matrigel, onto which PC3-cells (5×10^4/insert) were seeded in medium containing 10% FCS. Experiments were done with both, untransfected PC3 cells (visualized by Giemsa staining) and PC3 cells stably expressing GFP. After 24 hours, the medium in the upper and lower chamber was changed for phenol red- and FCS-free medium and cells were subjected to starvation for the next 24 hours. Thereafter, recombinant human MIF was added alone or in combination with antibodies (BaxB01, BaxG03, BaxM159, and isotype control antibody) to the lower chambers of the dish. Cells were allowed to migrate through the porous membrane for 24 hours. Thereafter, the medium was aspirated from the upper chamber, the Matrigel mechanically removed (with a forceps) from the membrane and the dish immersed in 4% paraformaldehyde for 20 minutes to fix cells. The membranes were cut out with a scalpel. GFP-expressing cells adhering to the lower face of the membrane were visualized by fluorescence microscopy. Fluorescence images were captured at a magnification of 100- or 400-fold. Data are expressed as the number of cells per visual field.

Animal experiments

Animal experiments were carried out in accordance with the guidelines of the Medical University of Vienna (Vienna, Austria; Good Scientific Practice Manual) and were approved by the Animal Welfare Committee of the Medical University of Vienna and the Austrian Science Ministry.

Anti-MIF antibodies were injected into MF-1 nude mice intravenously, subcutaneously and intraperitoneally ($n = 6$/group) to determine the pharmacokinetic parameters. Blood (0.05 mL) was drawn at predefined intervals (starting with 4 hours after injection up to day 6) into heparinized capillaries. Plasma was prepared by centrifugation. Antibody concentrations were determined by ELISA. Briefly, γ-chain–specific goat anti-human IgG was coated onto MaxiSorp ELISA plates. Plates were blocked with 1.5% fish gelatin in PBS. Plasma samples (diluted in 1.5% fish gelatin/PBS) were applied and incubated for 2 hours at 20°C. After washing, HRP-labeled Fc-specific goat anti-human IgG was added. The plates were incubated and washed. The 3,3′,5,5′-tetramethylbenzidine solution was added and the reaction stopped with H_2SO_4 after 30 minutes. Bound anti-MIF antibody was detected at 450 nm.

For xenografts, PC3 cells were harvested from exponentially growing cultures and mixed with growth factor–depleted Matrigel. The cell suspension (2×10^6 cells in 0.25 mL growth factor–depleted Matrigel) was injected subcutaneously into the right flank of male MF-1 nude mice. Treatment was started on the day after inoculation. MIF antibodies (BaxG03, BaxB01, and BaxM159) and the isotype-matched (IgG1) irrelevant human control antibody were administered every other day by intraperitoneal injection. Starting on day 14 after inoculation, the size of the xenograft tumors was measured every other day. Volumes were calculated according to $V = 0.5 \times a \times b^2$ (where a and b are the longest and shortest diameter, respectively). Animals were sacrificed typically after 30 days. Tumors were excised, measured, weighed, and fixed in 4% paraformaldehyde for staining and immunohistochemistry.

Histopathology

Fixed samples were embedded in paraffin. Paraffin blocks were cut into 4-μm thick sections and deparaffinated in ascending xylol. Adjacent sections from each tumor were stained with hematoxylin and eosin (H&E) or immunostained for Ki67. For immunohistochemistry, tissue sections were rehydrated and boiled in 0.01 mol/L citrate buffer, pH 6, for 2 minutes at and incubated for

Published OnlineFirst April 25, 2013; DOI: 10.1158/1535-7163.MCT-12-0988

10 minutes at 4°C. After cooling, the sections were treated sequentially with 3% H_2O_2 in PBS+Tween 20 for 15 minutes, the avidin/biotin–blocking system and the Mouse Ig Blocking Reagent according to the protocol of the manufacturer. The sections were incubated for 16 hours with the murine monoclonal antibody to human Ki67 at a 1:1,000 dilution. Immunoreactivity was revealed with the IDetect super stain system. The sections were then counterstained with Mayer's hematoxylin.

Statistical analysis

The distribution was tested with the Kolmogorov–Smirnov test. If the distribution was not skewed by outliers, the difference between group means was evaluated by ANOVA followed by Dunnett test for multiple comparisons. Otherwise, the data were evaluated by a Kruskal–Wallis test followed by Dunn *post hoc* test. If only 2 groups were compared, an unpaired *t* test was done. Concentration–response curves were subjected to nonlinear least curve fitting to the Hill-equation using a Marquardt–Levenberg algorithm. Pharmacokinetic data were fitted to the Bateman equation (for subcutaneous or intraperitoneal injection) or to equations for a mono- or biexponential decay (for intravenous injection).

Results

Addition of antibodies against MIF reduces growth of prostate cancer cells in culture

Human prostate cancer cell lines release MIF when cultivated in serum-free medium (23). We confirmed these finding by analyzing cell culture supernatant from PC3 cells by ELISA. We used human anti-MIF antibodies to verify if the released (and displayed) MIF acted via autocrine and paracrine loops to support cell growth and survival. PC3 cells were incubated with BaxG03 or with BaxB01 (Fig. 1A) for 24 hours, cell numbers were reduced by up to 40% with an EC_{50} of 7 ± 4 nmol/L and 5.5 ± 1.8 nmol/L for BaxG03 and BaxB01, respectively. In contrast, the isotype-matched control antibody (produced and purified under similar conditions) did not affect cell growth (Fig. 1A). BaxG03 was also tested in Du145 cells, where it inhibited cell proliferation with comparable efficacy and potency (Fig. 1B). Growth inhibition was similar in magnitude after 24 hours and 48 hours (insets in Fig. 1A and B). Consistent with earlier findings (26), we found that growth of the androgen-dependent prostate cancer cell lines LnCAP and VCAP was not inhibited by MIF-directed antibodies.

Anti-MIF antibodies reduce the level of active ERK1/2 and of active AKT

The antibody-induced reduction in cell number may arise from suppression of proliferative or survival signals provided by MIF. In fact, MIF seems to activate both limbs, because it may stimulate ERK1/2 and AKT (12, 14). We explored, if MIF also activated ERK1/2 phosphorylation in PC3 cells. Indeed, addition of MIF promoted the accumulation of phosphorylated ERK1/2 in a concentration-dependent manner (data not shown). We then verified that addition of anti-MIF antibodies (BaxG03, BaxM159, and BaxB01) reduced steady-state levels of ERK-phosphorylation in asynchronously growing cells maintained in the presence of FCS for 48 hours (Fig. 2A). The isotype-matched control antibody did not cause any appreciable effect on phosphorylated ERK1/2. Similar observations were made with the serine/threonine-kinase AKT (Fig. 2B). ERK and AKT phosphorylation was also reduced in DU145 but not in LnCAP cells treated with the antibodies (not shown). Taken together, our results suggested that (i) the autocrine/paracrine action of MIF supplied a substantial proportion of the signal required for sustained serum-induced phosphorylation of ERK1/2 and of AKT, and (ii) the human anti-MIF antibodies interfered with signal transduction that led to activation of ERK1/2 and AKT.

Caspase activation in PC3 cells incubated in the presence of anti-MIF antibodies

Active AKT supplies survival signals and suppresses programmed cell death by multiple mechanisms, including the direct phosphorylation (i.e., inactivation) of the proapoptotic BCL-2 family member BAD (29) and the initiator caspase-9 (30). Similarly, active ERK2 phosphorylates caspase-9 on threonine^{125} and this suppresses its activity (31). Reduced levels of active AKT and ERK1/2 are predicted to favor caspase activation and thus to promote apoptosis. Because steady-state levels of phospho-ERK1/2 were lowered, if PC3 cells were maintained in the presence of anti-MIF antibodies, we surmised that levels of phosphorylated caspase-9 were reduced. In fact, we observed a reduction of phospho-caspase-9 in the presence of the MIF-neutralizing antibody BaxG03 (Fig. 2C). Caspase-3 is the dominant effector caspase downstream of caspase-9. Accordingly, we measured the activity of caspase-3 in PC3 cells with a fluorogenic substrate. If PC3 cells were incubated with increasing concentrations of antibody BaxG03 for 48 hours, the lysates contained elevated levels of caspase activity (Fig. 3A). The specificity of the enzymatic reaction was confirmed by blocking caspase-3 with the inhibitor Ac-DEVD-CHO (Fig. 3A). The fluorescence levels measured at the end of the incubation period (after 180 minutes) were plotted to generate a dose–response curve and an EC_{50} of approximately 20 nmol/L for BaxG03 was estimated by fitting the data to a hyperbola (Fig. 3A, inset). Increased caspase-3 activation resulted from specific MIF inhibition by BAXG03, because the effect was reversed in the presence of excess recombinant MIF (Fig. 3B) and was not seen in the presence of control antibody (Fig. 3B, inset). Similar findings were obtained with BaxM159 (data not shown).

Anti-MIF antibodies inhibit MIF-mediated invasion of PC3 cells

To investigate the proinvasive activities of MIF on prostate cancer cells, PC3 cells were seeded in the upper

Published OnlineFirst April 25, 2013; DOI: 10.1158/1535-7163.MCT-12-0988

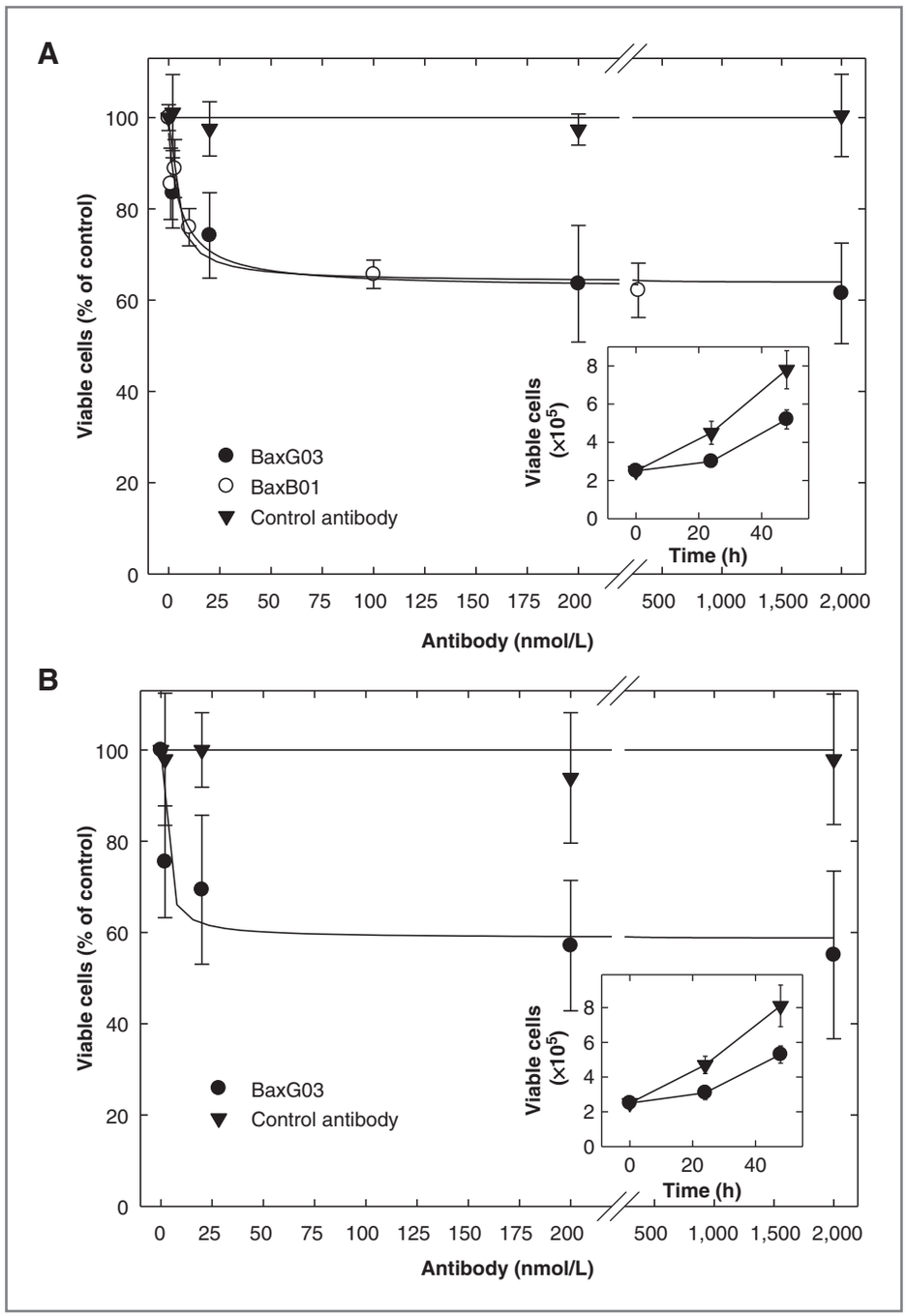

Figure 1. Growth inhibitory effects of anti-MIF antibodies on PC-3 and Du145 cells. Starved PC3 (A) or Du145 (B) cells were incubated with the indicated concentrations of monoclonal anti-MIF antibodies BaxG03, BaxB01, or the isotype-matched (IgG1) control antibody. The number of viable cells was determined after 24 hours of incubation. The control value (number of viable cells in the absence of antibody) was set 100% to normalize for interassay variations. Viable cell count is depicted as percentage of the control value as function of antibody concentration. In the inset, cells (2.5×10^6/wells) were allowed to proliferate in presence of 25 nmol/L control antibody and BaxBG03 for 24 and 48 hours. Data are mean $\pm$ SD from 3 independent experiments done in triplicate. The inhibition seen at antibody concentrations more than 10 nmol/L were statistically significant [(repeated measures ANOVA followed by Bonferroni *post hoc* test in A); *t* test for paired data in B and in the insets].

chamber on a Matrigel layer and then MIF was added to the lower chamber to attract the cells. The transmigration of PC3 cells through Matrigel was markedly enhanced when MIF was added to the lower chamber (Fig. 4A). The chemoattractant action of MIF was blocked by addition of anti-MIF antibodies BaxB01, BaxG03, or BaxM159 but not by the isotype control antibody (Fig. 4A). Several concentrations of MIF were tested to determine the concentration range at which MIF was effective as a chemoattractant. As can be seen from Fig. 4B, a bell-shaped concentration–response curve was obtained. The optimal signal-to-noise ratio was seen at 0.1 nmol/L MIF. Accordingly, we determined the apparent affinity of MIF-directed antibodies by monitoring the concentration required to antagonize the action of 0.1 nmol/L MIF. BaxG03, BaxB01, and BaxM159 inhibited the action of MIF with IC_{50} values in the range of 2 to 4 nmol/L (Fig. 4C). Differences between individual antibodies were modest and thus not statistically significant.

Published OnlineFirst April 25, 2013; DOI: 10.1158/1535-7163.MCT-12-0988

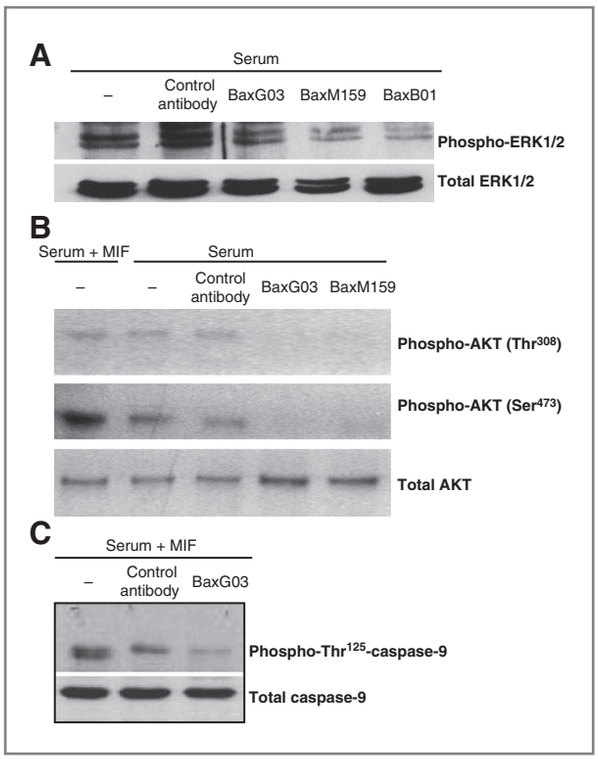

Figure 2. Treatment of PC3 cells with anti-MIF antibodies reduced the levels of phosphorylated ERK1/2, AKT, and caspase-9. Starved PC3 cells were incubated in the presence of 10% FCS, 10 nmol/L recombinant MIF, 100 nmol/L BaxG03, BaxB01, BaxM159, or isotype control antibody as indicated. Cell lysates were separated by SDS-PAGE and blotted on nitrocellulose membranes and the phosphorylated form of ERK1/2 (A), AKT (B), or the T^{125}-phosphorylated form of caspase-9 (C) were visualized with phospho-specific antisera. The total levels of the enyzmes were determined by using antisera that recognized all forms of the enzymes and were visualized as a loading control. Data are representative of at least 2 independent experiments.

Pharmacokinetics of anti-MIF antibodies

Before examining the actions of the antibodies *in vivo*, we determined their pharmacokinetics to define the optimal dosing interval. The antibodies were first administered to MF1 nude mice by intravenous injection and blood was taken at different time points for analysis. The result of this analysis is shown in Supplementary Fig. S1A for BaxG03. Regardless of whether BaxG03 was administered at 20, 50, or 100 mg/kg, an initial rapid decline was followed by a protracted second elimination phase after intravenous injection. The fit to a biexponential decay was significantly better than to a monoexponential decay ($P < 0.01$; F test based on the extra-sum-of-squares principle). The concentrations at time 0 in the central compartment (C_{01}) and in the peripheral compartment (C_{02}) were calculated from the 2-compartment model. These increased in a linear manner with antibody dose (Supplementary Fig. S1B). This dose linearity allowed for the calculation of the volumes of distribution (V_D). These were on average 1.3 and 6.1 mL for the central and the peripheral compartment, respectively. In a mouse of approximately 25 to 30 g, these volumes are consistent with the plasma volume (5% of body weight) and the volume of the extracellular space (~20% of body weight). In contrast, the elimination constants k_{e1} and k_{e2} were independent of dose. Half-lives were calculated from the individual k_{e1} and k_{el2} values and amounted to 5 to 8 hours for the initial elimination phase and 65 to 90 hours for the second elimination phase from the 2 compartments. We also determined the kinetics after intraperitoneal administration (Supplementary Fig. S1C); BAXG03 was rapidly absorbed after intraperitoneal administration ($k_{abs} = 1.13\ h^{-1}$). A half-life of approximately 58 hours was calculated for the declining phase. It is worth noting that these half-lives were estimated from a fit to a simple Bateman equation, that is, to the sum of an exponential rise and a concomitant exponential decay. We did not attempt to account for a biphasic exponential decay, because the number of estimated parameters (i.e., 6) would not have been commensurate with the number of available data points (i.e., 9). Thus, the half-life estimated after intraperitoneal administration represents the overall half-life of the rapid distribution phase and the slower elimination phase resolved after intravenous administration. Consistent with its rapid absorption, the bioavailability of BAXG03 was high after intraperitoneal injection (i.e., 72.3% calculated from the ratio intraperitoneal area under the curve $(AUC)_{0-6d}$/intravenous $AUC_{0-6d} \times 100$; >90% for $AUC_{0-\infty}$). A similar analysis was done for BaxB01 after intraperitoenal injection, which gave analogous results (i.e., an overall half-life for the declining phase in the range of 50 hours and a bioavailability >70% and >90% for AUC_{0-6d} and $AUC_{0-\infty}$, respectively). On the basis of these observations, we concluded that (i) the antibodies reached the extracellular compartment, (ii) that the intraperitoneal route resulted in adequate systemic exposure, and (iii) that a dosing interval of every other day ought to lead to effective steady state antibody concentrations in the high nanomolar range.

Anti-MIF antibodies reduce the growth of PC3 xenograft tumors in MF-1 nude mice

The data summarized earlier suggest that anti-MIF antibodies may inhibit growth of prostate cancer *in vivo*. We used a xenograft model to provide a proof-of-principle. Male nude MF1 mice were subcutaneously inoculated with 2×10^6 PC3 cells suspended in Matrigel. Treatment by intraperitoneal injection of antibodies was initiated on the next day and continued every other day for 4 weeks. The administration of 40 mg/kg BaxG03 effectively reduced tumor growth relative to the isotype control antibody (Fig. 5A). These findings were verified upon excision of the tumors after 30 days, measuring the size of the tumors for calculating the volume (Fig. 5B) and weighing the tumors (Fig. 5C). Tumor volumes calculated from the dimensions of each individual tumor were reasonably similar to the measured weight. Figure 5B and C document that the inhibitory effect of BaxG03 on tumor growth resulted in a statistically significant reduction

Published OnlineFirst April 25, 2013; DOI: 10.1158/1535-7163.MCT-12-0988

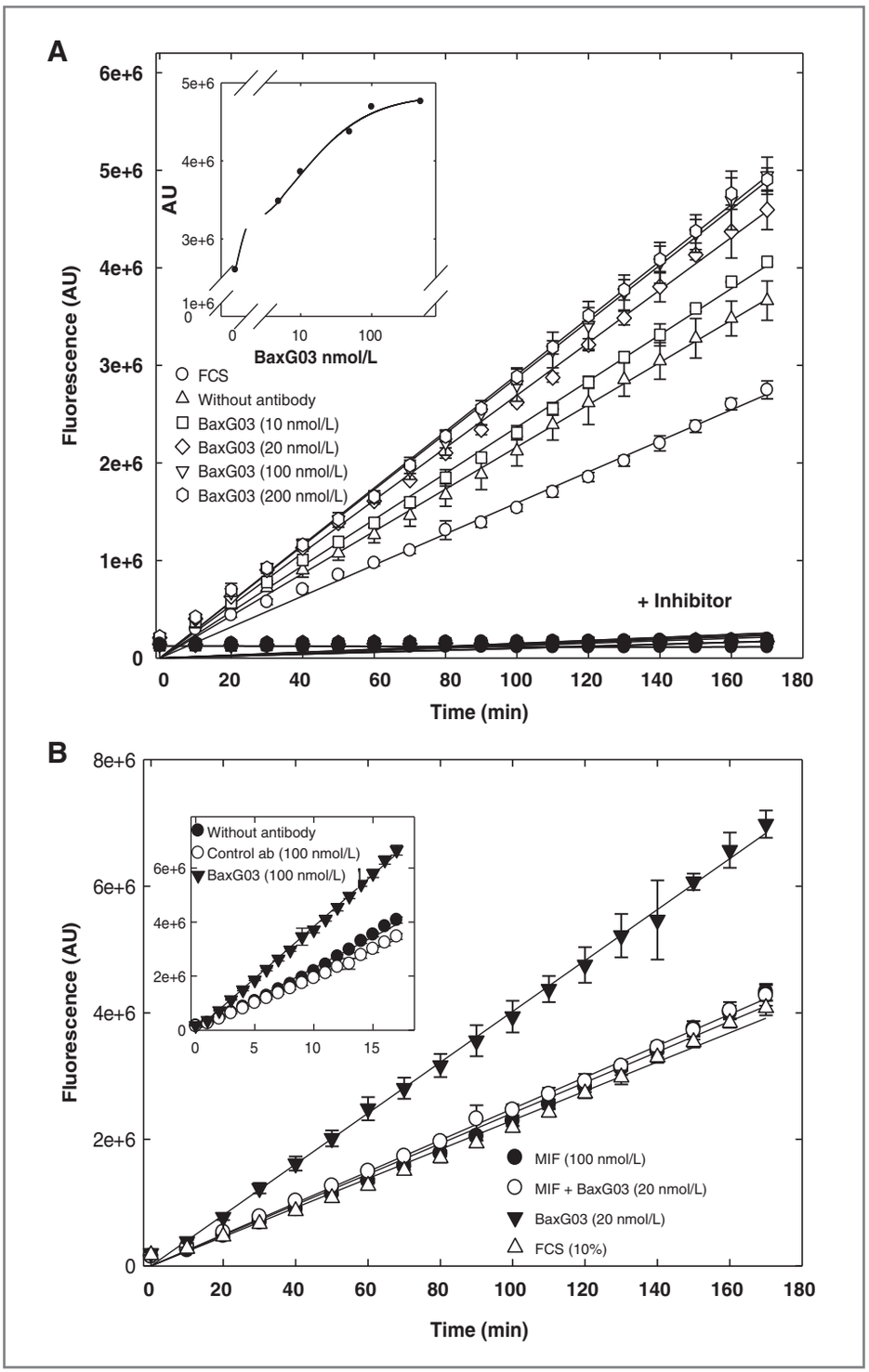

Figure 3. Activation of caspase-3 by BaxG03 in PC3 cells. A, PC3 cells were incubated in 10% FCS, either without antibody or in the presence of BaxG03 at the indicated concentrations. Caspase-3 activity was determined in the cell lysates using Ac-DEVD-AFC fluorogenic substrate and the arbitrary fluorescence units (AU) were plotted against time (open symbols). An aliquot of each lysate was preincubated with the irreversible caspase-3 inhibitor Ac-DEVD-CHO before addition of the fluorogenic substrate (closed symbols, curves labeled + inhibitor). The inset in A is a replot of the fluorescence recorded after 180 minutes as a function of the concentration of BaxG03 to yield a concentration–response curve. B, PC3 cells were incubated in 10% FCS, either without additive or in presence of BaxG03 or recombinant MIF at indicated concentrations. Again, the arbitrary fluorescence units (AU) were plotted against time. The inset in B documents that the control antibody (control ab) did not cause any appreciable increased caspase activity. Data are mean ± SD ($n = 3$). The slopes of the regression lines observed in the presence of ≥20 nmol/L BaxG03 differed in a statistically significant manner from those seen in the presence of FCS, control antibody, or the combination of BaxG03+MIF (repeated measures ANOVA followed by Bonferroni *post hoc* test).

in tumor size. This conclusion was also supported by the microscopic examination of histologic sections. As exemplified in Fig. 5D, tumors from BaxG03-treated animals contained large eosinophilic areas of low cell content. In contrast, xenografts from animals treated with an isotype control antibody were characterized by a dense accumulation of cells (resulting in uniform distribution of blue nuclei).

A similar approach was used to examine the dose-dependent inhibition of tumor growth by BaxG03 and the data are summarized in Fig. 6A. From the dose–response curve (shown as inset in Fig. 6A), we estimated

Published OnlineFirst April 25, 2013; DOI: 10.1158/1535-7163.MCT-12-0988

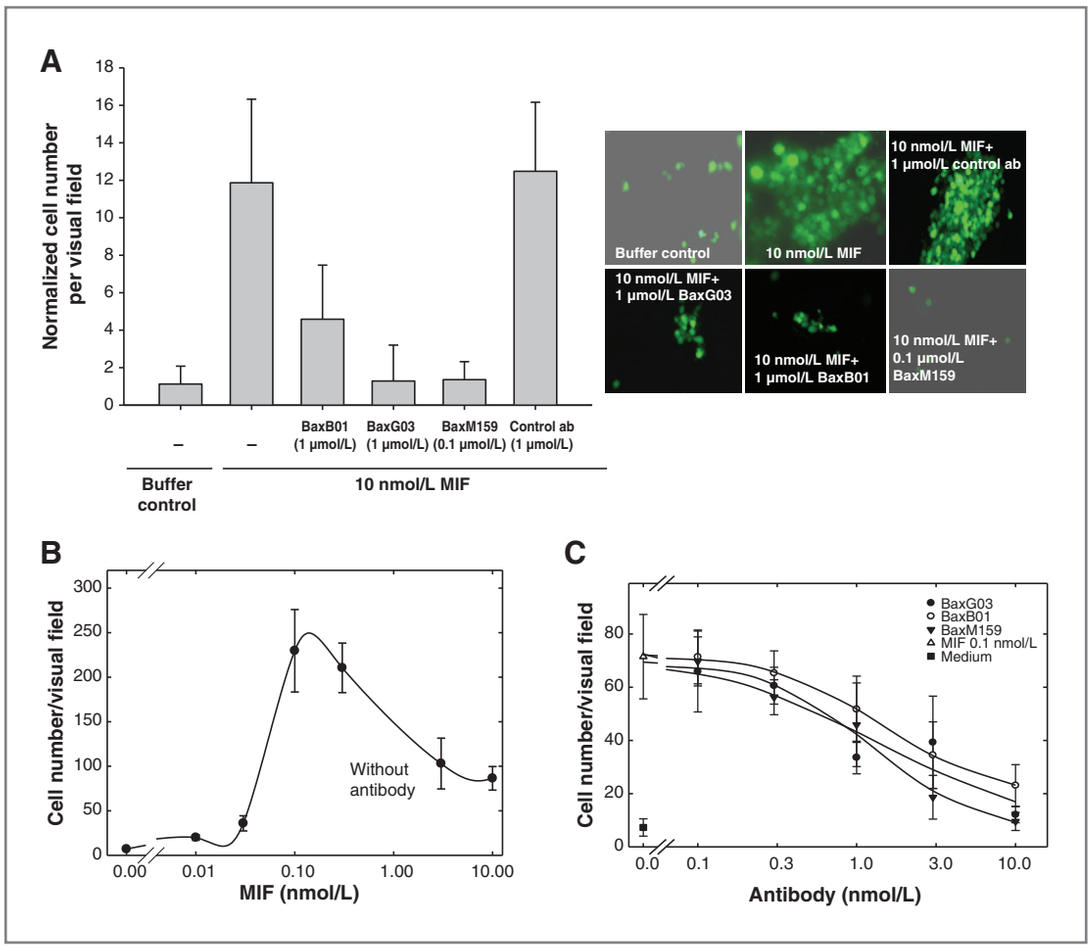

Figure 4. Anti-MIF antibodies reduced the invasion and migration of PC3 cells through Matrigel-coated microporous membranes. Human recombinant MIF was added at the indicated concentrations to the lower chamber and serum-starved PC3 cells that stably expressed GFP were allowed to migrate through Matrigel-coated microporous membranes. A, the chemoattractant activity of recombinant MIF (10 nmol/L) was reduced by addition of the indicated concentrations of BaxB01, BaxG03, and BaxM159 to the lower chambers. An isotype control antibody (control ab) was used as negative control. Left, the normalized cell number per visual field; right, representative fluorescence images at a 100-fold magnification. B, concentration–response curve for the chemoattractant activity of recombinant human MIF. The cell number per visual field is shown in relation to the exogenous recombinant MIF concentration. C, concentration–response curves for the inhibition of the chemoattractant activity of 0.1 nmol/L MIF by the anti-MIF antibodies. The curves were generated by subjecting the data to nonlinear fitting to the Hill-equation. Data are mean ± SD from 2 (A) and 3 (B and C) independent experiments. In C, the values observed in the presence of 0.1 nmol/L in combination with ≥1 nmol/L BaxG03, BaxB01, and BaxM159 differed in a statistically significant manner from those seen in the sole presence of 0.1 nmol/L MIF (repeated measures ANOVA followed by Bonferroni *post hoc* test).

an ED_{50} of 14 mg/kg. The tumor xenografts were evaluated microscopically and proliferating cells were stained for Ki67 immunoreactivity (insets in Fig. 6B). This investigation showed that even the lowest dose of 10 mg/kg BAXG03 clearly reduced the number of cells in the xenograft (cf., insets in Fig. 6B). If the number of Ki67-positive cells (brown cells) in the tumor sections were counted in randomly selected visual fields, tumors excised from BaxG03-treated animals contained a significantly lower number of Ki67-positive cells (Fig. 6B). The resulting dose–response relation was similar to that depicted in Fig. 6A with the ED_{50} estimate of 8.5 mg/kg. We also determined the plasma concentrations of BaxG03 at the end of the experiment. These trough concentrations (Supplementary Fig. S2) were in a range consistent with the pharmacokinetics, that is, about half the concentration of C_{02} (cf., open circles in Supplementary Fig. S1B) and within the range predicted from the Bateman curve obtained after intraperitoneal injection (cf., Supplementary Fig. S1C).

We also evaluated BaxB01 and BaxM159 for their capacity to inhibit the growth of PC3 xenografts in a dose-dependent manner. Both antibodies were effective in suppressing the growth of the xenograft tumors over a comparable dose range, that is, the administration of doses in the range between 15 and 40 mg/kg resulted in a statistically significant reduction of tumor weight (Supplementary Figs. S2 and S3). We also subjected these tumor samples to histologic analysis; the resulting stainings with H&E and the immunocytochemistry for Ki67

Published OnlineFirst April 25, 2013; DOI: 10.1158/1535-7163.MCT-12-0988

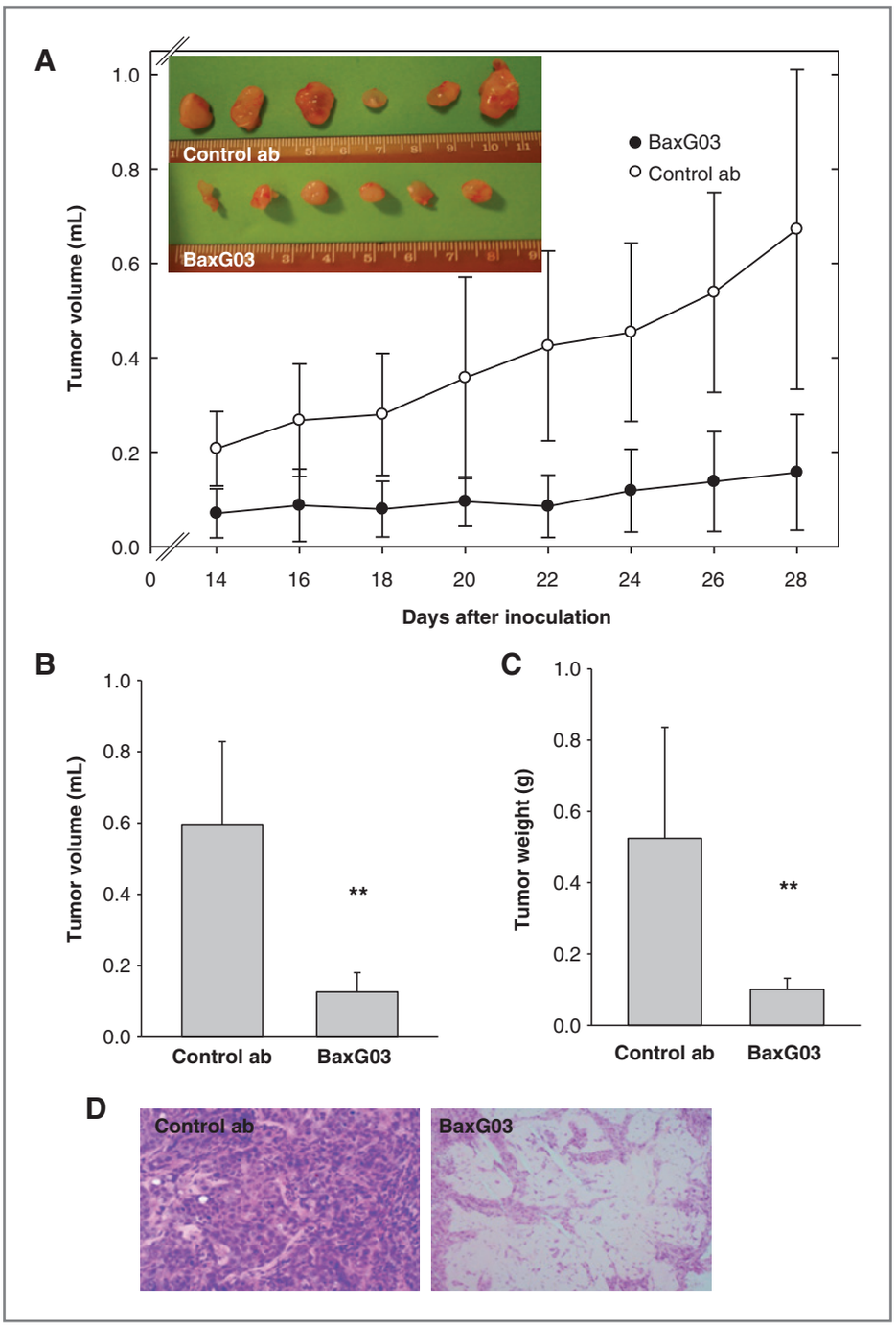

Figure 5. BaxG03 reduces the growth of PC3 xenograft tumors. MF1 nude mice were inoculated with PC3 cells and the animals were treated with BaxG03 or isotype control antibody (1.6 mg/mouse, i.e., 40 mg/kg) by intraperitoneal injection every other day. The tumor volume was measured every other day from day 14 until day 28 and the resultant growth curves are depicted (A). On day 30, after cell injection the mice were sacrificed, tumor xenografts were dissected, excised and photographed (inset in A). The size of the tumor xenografts was measured to recalculate the volume (B) and the tumors were weighed (C). Two representative H&E–stained histologic sections from tumors of each treatment regimen are shown (E). Data are expressed as mean ± SD ($n = 6$). **, $P < 0.01$.

gave results that were comparable with those exemplified earlier for BaxG03 (data not shown).

Discussion

High levels of circulating MIF are found in human prostate cancer and predict poor prognosis (23, 24). Suppression of MIF production by RNA interference or blocking of MIF with polyclonal anti-MIF antibodies reduces the growth of androgen-independent prostate cancer cells *in vitro* (26). However, these experiments did not address the question, if neutralizing extracellular MIF by a monoclonal antibody is a viable strategy to block the growth of prostate cancer cells *in vivo*. It was also *a priori* not clear, if MIF-directed antibodies can penetrate into tumor tissue to an extent that suffices to block the actions of MIF. Our

Published OnlineFirst April 25, 2013; DOI: 10.1158/1535-7163.MCT-12-0988

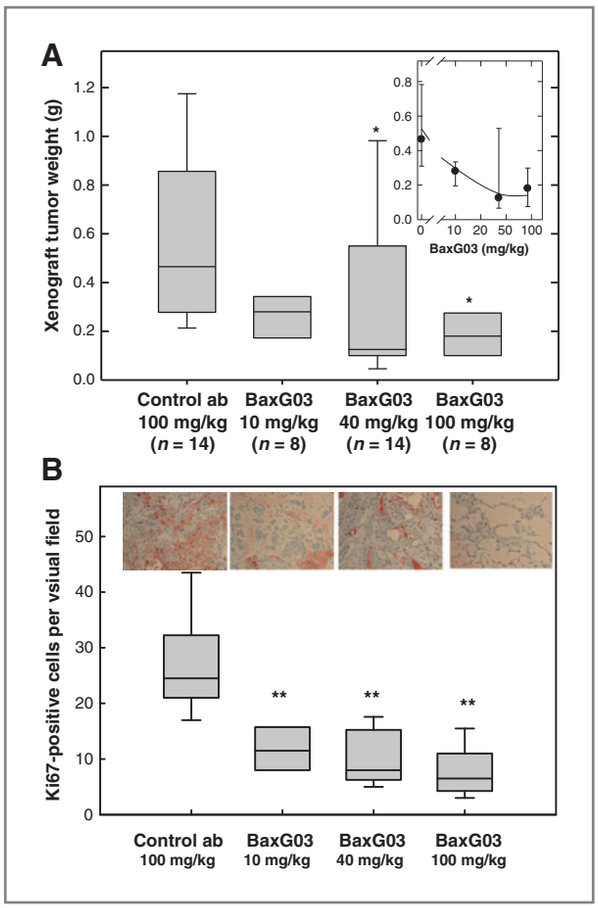

Figure 6. Dose-dependent inhibition of xenograft outgrowth by BaxG03. MF1 nude mice were inoculated with PC3 cells and the animals were treated with BaxG03 or isotype control antibody at indicated doses every other day for 28 days. A, the box plot shows the median xenograft tumor weight, the boxed area and the whiskers the 25% to 75% and the 5% to 95% percentile, respectively. In the inset, the median data have been replotted to generate a dose–response curve; the error bars delineate the 95% confidence interval. The weight of the xenografts was significantly smaller in the groups treated with BaxG03 at 40 and 100 mg/kg than in the control antibody-treated animals. The numbers of animals per group are indicated (*n*). *, $P < 0.05$ from control. B, tumor sections obtained from animals treated with different doses of BaxG03 and control antibody were stained for Ki67. Representative photomicrographs (40-fold magnification) are shown as insets. Five to 7 randomly selected visual fields were counted (at a 100-fold magnification) per tumor section from each animal. The box plot shows the median number of Ki67-positive cells per visual field, the 25% to 75% percentile as boxed area, and the whiskers the 5% to 95% percentile. All treatment groups were significantly different from the isotype control group. **, $P < 0.01$.

experiments were designed to address these questions and provide a proof-of-principle: (i) *in vitro*, the human prostate cancer cell line PC3 relies in part on an autocrine/paracrine action of MIF, which was abrogated by the antibodies. (ii) Mechanistically, the antibodies abrogated MIF-dependent proliferation and survival signaling pathways, that is, stimulation of ERK1/2- and AKT-phosphorylation, and thus favored the activation of programmed cell death, that is, the accumulation of active caspase-3. (iii) Similarly, the antibodies effectively inhibited the capacity of prostate cancer cells to invade and migrate through extracellular matrix components. (iv) The pharmacokinetic parameters justified the assumption that the antibodies also permeated into the interstitial fluid. (v) Accordingly, the antibodies also suppressed the growth of human prostate cancer cell xenografts.

We have recently described the generation of human anti-MIF antibodies that neutralize biologic MIF activities (28). Herein, we report the effectiveness of these human anti-MIF antibodies in a xenograft model of human cancer cells. Previous experiments focused on murine models with the syngenic colon cancer cell line CT26 that were treated with goat or rabbit anti-MIF antiserum (23, 29). To the best of our knowledge, a comprehensive analysis of the pharmacodynamics and pharmacokinetics of anti-MIF antibodies has not yet been done; our experiments are the first to provide the pertinent data. *In vitro*, half-maximum inhibition of cell proliferation and cell migration was seen in the range of about 2 to 10 nmol/L. This was also the concentration range required for activating caspase-3. The biexponential decay observed after intravenous administration allowed for estimating the concentration initially present in the peripheral compartment. The extrapolated concentrations were in the range of 0.6 to 2 μmol/L. The estimated volume of the peripheral compartment was within the range expected for the extracellular space. Hence, it was reasonable to surmise that within the dose range tested—i.e., 5 to 100 mg/kg—the antibodies reached effective concentrations within the interstitial fluid surrounding the tumor cells. In fact, the ED_{50} was estimated in the range of 8 to 14 mg/kg, and thus consistent with the predictions from the pharmacokinetic analysis.

Three strategies can be envisaged to antagonize the actions of MIF: (i) neutralizing MIF activity by monoclonal antibodies, (ii) blocking MIF by low-molecular weight inhibitors (26, 32–35), and (iii) blocking MIF-receptors. Blockage of MIF-receptors has not been explored in detail. Conceptually, this approach suffers from the drawback that all candidate MIF-receptors have additional ligands. Although CXCR2 is involved in angiogenesis, tumorigenicity, and metastasis of PC3 cells implanted orthotopically in nude mice (36), receptor inhibitors are likely to disrupt other crucial responses: antagonism of CXCR2 interferes with recruitment of neutrophils to the site of bacterial infections by IL-8. Analogous considerations apply to the other MIF receptors, namely CXCR4 (8) and CXCR7 (10). CD74 is the invariant chain of the MHC class II molecule and its downregulation is likely to have additional effects (37, 38). In addition, in some instances, cells that lack CD74 are nevertheless responsive to MIF (22).

Compounds that bind to and inhibit the tautomerase activity of MIF were proposed as an alternative strategy to blunt the actions of MIF (32). These compounds elicit

Published OnlineFirst April 25, 2013; DOI: 10.1158/1535-7163.MCT-12-0988

beneficial effects in models of inflammatory disease (33, 34). However, it seems questionable that tautomerase activity is important for mediating the growth promoting effects of MIF: the genetically engineered knockin of an allele encoding a tautomerase-deficient MIF did not eliminate the growth promoting action of the protein (7). Tautomerase inhibitors of MIF may confer their inhibitory properties by interfering with the binding of MIF to CD74 rather than by inhibition of enzymatic activity (35).

The antibodies described here recognize distinct epitopes in the 115 residues of MIF. BaxG03 and its variant BaxM159 bind to the C-terminus (amino acids 86–102) and BaxB01 binds in the vicinity of the MIFs oxidoreductase motif (residues 50–68; ref. 28). In the three-dimensional structure these epitopes are juxtaposed. We also tested antibody BaxH02 that is specific for a structural epitope of MIF. BaxH02 neutralized MIF-induced cell proliferation and MIF's glucocorticoid overriding activity *in vitro*. Interestingly, this antibody failed to cause significant inhibition in the PC3 xenograft model, thus confirming the observation described previously that only antibodies specific for regions aa50-68 or aa86-102 exert a beneficial effect *in vivo* (28). The MIF antibodies used neither induce complement-dependent cell lysis of MIF-responsive cells nor antibody-dependent cellular cytotoxicity (Douillard and colleagues, unpublished data).

MIF is produced by a large number of cells (11, 15), nevertheless high doses of anti-MIF antibodies were tolerated by the mice over a 4-week period without any frank toxicity in both, the present study and earlier reports (39, 40). Similarly, genetic deletion of MIF does not have any major detrimental effects as MIF-deficient mice are viable, fertile and do not have any overt abnormalities (41). In fact, their lifespan is extended (42). Thus, a therapeutic strategy that targets MIF in cancer seems justified. The human anti-MIF antibodies described here may represent promising candidates.

Disclosure of Potential Conflicts of Interest

M. Freissmuth has commercial research grant from Baxter and is a consultant/advisory board member of the same. H. Ehrlich is employed as Vice President, Global R&D by Baxter and has ownership interest (shareholder and IP holder; including patents) in the same. F. Scheiflinger has ownership interest (including patents) in Baxter BioScience. R.J. Kerschbaumer has ownership interest (including patents) in Baxter Healthcare. No potential conflicts of interest were disclosed by the other authors.

Authors' Contributions

Conception and design: M. Freissmuth, D. Völkel, M. Thiele, P. Douillard, F. Scheiflinger, R.J. Kerschbaumer
Development of methodology: D. Völkel, P. Douillard, F. Scheiflinger
Acquisition of data (provided animals, acquired and managed patients, provided facilities, etc.): F. Hussain, D. Völkel, P. Douillard, P. Thurner, H. Ehrlich
Analysis and interpretation of data (e.g., statistical analysis, biostatistics, computational analysis): F. Hussain, D. Völkel, M. Thiele, P. Douillard, P. Thurner, H. Ehrlich, F. Scheiflinger, R.J. Kerschbaumer
Writing, review, and/or revision of the manuscript: F. Hussain, M. Freissmuth, D. Völkel, M. Thiele, P. Douillard, H. Ehrlich, H.-P. Schwarz, F. Scheiflinger, R.J. Kerschbaumer
Administrative, technical, or material support (i.e., reporting or organizing data, constructing databases): F. Hussain, M. Freissmuth, D. Völkel, P. Douillard, G. Antoine
Study supervision: M. Freissmuth, D. Völkel, P. Douillard, H. Ehrlich, F. Scheiflinger, R.J. Kerschbaumer

Grant Support

F. Hussain was supported by a stipend from the Pakistani Higher Education Commission.

The costs of publication of this article were defrayed in part by the payment of page charges. This article must therefore be hereby marked *advertisement* in accordance with 18 U.S.C. Section 1734 solely to indicate this fact.

Received October 10, 2012; revised April 19, 2013; accepted April 22, 2013; published OnlineFirst April 25, 2013.

References

1. Bloom BR, Bennett B. Mechanism of a reaction *in vitro* associated with delayed-type hypersensitivity. Science 1966;153:80–2.
2. David JR. Delayed hypersensitivity *in vitro*: its mediation by cell-free substances formed by lymphoid cell-antigen interaction. Proc Natl Acad Sci U S A 1966;56:72–7.
3. Merk M, Baugh J, Zierow S, Leng L, Pal U, Lee SJ, et al. The Golgi-associated protein p115 mediates the secretion of macrophage migration inhibitory factor. J Immunol 2009;182:6896–906.
4. Thiele M, Bernhagen J. Link between macrophage migration inhibitory factor and cellular redox regulation. Antioxid Redox Signal 2005;7:1234–48.
5. Bendrat K, Al-Abed Y, Callaway DJ, Peng T, Calandra T, Metz CN, et al. Biochemical and mutational investigations of the enzymatic activity of macrophage migration inhibitory factor. Biochemistry 1997;36:15356–62.
6. Fingerle-Rowson G, Kaleswarapu DR, Schlander C, Kabgani N, Brocks T, Reinart N, et al. A tautomerase-null macrophage migration-inhibitory factor (MIF) gene knock-in mouse model reveals that protein interactions and not enzymatic activity mediate MIF-dependent growth regulation. Mol Cell Biol 2009;29:1922–32.
7. Shi X, Leng L, Wang T, Wang W, Du X, Li J, et al. CD44 is the signaling component of the macrophage migration inhibitory factor-CD74 receptor complex. Immunity 2006;25:595–606.
8. Bernhagen J, Krohn R, Lue H, Gregory JL, Zernecke A, Koenen RR, et al. MIF is a noncognate ligand of CXC chemokine receptors in inflammatory and atherogenic cell recruitment. Nat Med 2007;13:587–96.
9. Weber C, Kraemer S, Drechsler M, Lue H, Koenen RR, Kapurniotu A, et al. Structural determinants of MIF functions in CXCR2-mediated inflammatory and atherogenic leukocyte recruitment. Proc Natl Acad Sci U S A 2008;105:16278–83.
10. Tarnowski M, Grymula K, Liu R, Tarnowska J, Drukala J, Ratajczak J, et al. Macrophage migration inhibitory factor is secreted by rhabdomyosarcoma cells, modulates tumor metastasis by binding to CXCR4 and CXCR7 receptors and inhibits recruitment of cancer-associated fibroblasts. Mol Cancer Res 2010;8:1328–43.
11. Noels H, Bernhagen J, Weber C. Macrophage migration inhibitory factor: a noncanonical chemokine important in atherosclerosis. Trends Cardiovasc Med 2009;19:76–86.
12. Lue H, Thiele M, Franz J, Dahl E, Speckgens S, Leng L, et al. Macrophage migration inhibitory factor (MIF) promotes cell survival by activation of the Akt pathway and role for CSN5/JAB1 in the control of autocrine MIF activity. Oncogene 2007;26:5046–59.
13. Kleemann R, Hausser A, Geiger G, Mischke R, Burger-Kentischer A, Flieger O, et al. Intracellular action of the cytokine MIF to modulate AP-1 activity and the cell cycle through Jab1. Nature 2000;408:211–6.
14. Mitchell RA, Metz CN, Peng T, Bucala R. Sustained mitogen-activated protein kinase (MAPK) and cytoplasmic phospholipase A2 activation by macrophage migration inhibitory factor (MIF). Regulatory role in

Published OnlineFirst April 25, 2013; DOI: 10.1158/1535-7163.MCT-12-0988

cell proliferation and glucocorticoid action. J Biol Chem 1999;274: 18100–6.
15. Mitchell RA. Mechanisms and effectors of MIF-dependent promotion of tumourigenesis. Cell Signal 2004;16:13–9.
16. Hudson JD, Shoaibi MA, Maestro R, Carnero A, Hannon GJ, Beach DH. A proinflammatory cytokine inhibits p53 tumor suppressor activity. J Exp Med 1999;190:1375–82.
17. Ren Y, Chan HM, Li Z, Lin C, Nicholls J, Chen CF, et al. Upregulation of macrophage migration inhibitory factor contributes to induced N-Myc expression by the activation of ERK signaling pathway and increased expression of interleukin-8 and VEGF in neuroblastoma. Oncogene 2004;23:4146–54.
18. Hagemann T, Robinson SC, Thompson RG, Charles K, Kulbe H, Balkwill FR. Ovarian cancer cell-derived migration inhibitory factor enhances tumor growth, progression, and angiogenesis. Mol Cancer Ther 2007;6:1993–2002.
19. Schoenfeld J, Jinushi M, Nakazaki Y, Wiener D, Park J, Soiffer R, et al. Active immunotherapy induces antibody responses that target tumor angiogenesis. Cancer Res 2010;70:10150–60.
20. Oda S, Oda T, Nishi K, Takabuchi S, Wakamatsu T, Tanaka T, et al. Macrophage migration inhibitory factor activates hypoxia-inducible factor in a p53-dependent manner. PLoS ONE 2008;3:e2215.
21. Hagemann T, Wilson J, Kulbe H, Li NF, Leinster DA, Charles K, et al. Macrophages induce invasiveness of epithelial cancer cells via NF-kappa B and JNK. J Immunol 2005;175:1197–205.
22. Krockenberger M, Dombrowski Y, Weidler C, Ossadnik M, Hönig A, Häusler S, et al. Macrophage migration inhibitory factor contributes to the immune escape of ovarian cancer by down-regulating NKG2D. J Immunol 2008;180:7338–48.
23. Meyer-Siegler KL, Iczkowski KA, Vera PL. Further evidence for increased macrophage migration inhibitory factor expression in prostate cancer. BMC Cancer 2005;5:73.
24. Muramaki M, Miyake H, Yamada Y, Hara I. Clinical utility of serum macrophage migration inhibitory factor in men with prostate cancer as a novel biomarker of detection and disease progression. Oncol Rep 2006;15:253–7.
25. Meyer-Siegler KL, Vera PL, Iczkowski KA, Bifulco C, Lee A, Gregersen PK, et al. Macrophage migration inhibitory factor (MIF) gene polymorphisms are associated with increased prostate cancer incidence. Genes Immun 2007;8:646–52.
26. Meyer-Siegler KL, Iczkowski KA, Leng L, Bucala R, Vera PL. Inhibition of macrophage migration inhibitory factor or its receptor (CD74) attenuates growth and invasion of DU-145 prostate cancer cells. J Immunol 2006;177:8730–9.
27. Verjans E, Noetzel E, Bektas N, Schütz AK, Lue H, Lennartz B, et al. Dual role of macrophage migration inhibitory factor (MIF) in human breast cancer. BMC Cancer 2009;9:230.
28. Kerschbaumer RJ, Rieger M, Völkel D, Le Roy D, Roger T, Garbaraviciene J, et al. Neutralization of macrophage migration inhibitory factor (MIF) by fully human antibodies correlates with their specificity for the β-sheet structure of MIF. J Biol Chem 2012;287:7446–55.
29. Kitazumi I, Tsukahara M. Regulation of DNA fragmentation: the role of caspases and phosphorylation. FEBS J 2011;278:427–41.
30. Cardone MH, Roy N, Stennicke HR, Salvesen GS, Franke TF, Stanbridge E, et al. Regulation of cell death protease caspase-9 by phosphorylation. Science 1998;282:1318–21.
31. Allan LA, Morrice N, Brady S, Magee G, Pathak S, Clarke PR. Inhibition of caspase-9 through phosphorylation at Thr^{125} by ERK MAPK. Nat Cell Biol 2003;5:647–54.
32. Lubetsky JB, Dios A, Han J, Aljabari B, Ruzsicska B, Mitchell R, et al. The tautomerase active site of macrophage migration inhibitory factor is a potential target for discovery of novel anti-inflammatory agents. J Biol Chem 2002;277:24976–82.
33. Crichlow GV, Cheng KF, Dabideen D, Ochani M, Aljabari B, Pavlov VA, et al. Alternative chemical modifications reverse the binding orientation of a pharmacophore scaffold in the active site of macrophage migration inhibitory factor. J Biol Chem 2007;282:23089–95.
34. Al-Abed Y, Dabideen D, Aljabari B, Valster A, Messmer D, Ochani M, et al. ISO-1 binding to the tautomerase active site of MIF inhibits its pro-inflammatory activity and increases survival in severe sepsis. J Biol Chem 2005;280:36541–4.
35. Cournia Z, Leng L, Gandavadi S, Du X, Bucala R, Jorgensen WL. Discovery of human macrophage migration inhibitory factor (MIF)-CD74 antagonists via virtual screening. J Med Chem 2009;52: 416–24.
36. Sun JK, Uehara H, Karashima T, Mccarty M, Shih N, Fidler IJ. Expression of interleukin-8 correlates with angiogenesis, tumorigenicity, and metastasis of human prostate cancer cells implanted orthotopically in nude mice. Neoplasia 2001;3:33–42.
37. Bakke O, Dobberstein B. MHC class II-associated invariant chain contains a sorting signal for endosomal compartments. Cell 1990;63: 707–16.
38. Roche PA, Teletski CL, Stang E, Bakke O, Long EO. Cell surface HLA-DR-invariant chain complexes are targeted to endosomes by rapid internalization. Proc Natl Acad Sci U S A 1993;90:8581–5.
39. Ogawa H, Nishihira J, Sato Y, Kondo M, Takahashi N, Oshima T, et al. An antibody for macrophage migration inhibitory factor suppresses tumour growth and inhibits tumour-associated angiogenesis. Cytokine 2000;12:309–14.
40. He XX, Chen K, Yang J, Li XY, Gan HY, Liu CY, et al. Macrophage migration inhibitory factor promotes colorectal cancer. Mol Med 2009;15:1–10.
41. Bozza M, Satoskar AR, Lin G, Lu B, Humbles AA, Gerard C, et al. Targeted disruption of migration inhibitory factor gene reveals its critical role in sepsis. J Exp Med 1999;189:341–6.
42. Harper JM, Wilkinson JE, Miller RA. Macrophage migration inhibitory factor-knockout mice are long lived and respond to caloric restriction. FASEB J 2010;24:2436–42.

Published OnlineFirst April 25, 2013; DOI: 10.1158/1535-7163.MCT-12-0988

Molecular Cancer Therapeutics

Human Anti-Macrophage Migration Inhibitory Factor Antibodies Inhibit Growth of Human Prostate Cancer Cells *In Vitro* and *In Vivo*

Filza Hussain, Michael Freissmuth, Dirk Völkel, et al.

Mol Cancer Ther 2013;12:1223-1234. Published OnlineFirst April 25, 2013.